Adipocyte Fatty Acid-Binding Protein: Interaction with Phospholipid Membranes and Thermal Stability Studied by FTIR Spectroscopy†

Arne Gericke,‡ Elizabeth R. Smith,§,|| David J. Moore,‡,⊥ Richard Mendelsohn,*,‡ and Judith Storch*,§

Department of Chemistry, Rutgers University, Newark, New Jersey 07102, and Department of Nutritional Sciences, Rutgers University, New Brunswick, New Jersey 08903

Received March 24, 1997; Revised Manuscript Received May 8, 1997⊗

ABSTRACT: Fatty acid-binding proteins (FABPs) found in many tissues constitute a family of low molecular weight proteins that are suggested to function as intracellular transporters of fatty acids. Studies of the transfer kinetics of fluorescent anthroyloxy-labeled long-chain fatty acids from FABP to model membranes led to the suggestion that the FABPs, typically considered to be cytosolic proteins, could nevertheless interact directly with membranes [Wootan, M. G., et al. (1993) *Biochemistry 32,* 8622−8627]. In the current study, the interaction of the adipocyte FABP (A-FABP) with vesicles of various phospholipids has been directly measured and confirmed with FTIR spectroscopy. The strength of this interaction was inferred from the lowering of the gel−liquid-crystal phase transition temperature as monitored from temperature-induced variations in the acyl chain CH_2 stretching frequencies and from the intensities of the components of the CH_2 wagging progressions. A-FABP interacts more strongly with anionic phospholipids (phosphatidylserine and cardiolipin) than with zwitterionic phosphatidylcholine. Unsaturation in the acyl chains leads to a greater reduction in T_m (stronger lipid−protein interaction). In contrast, neutralization of A-FABP surface charges by acetylation considerably weakens the interaction. Comparison of the shifts in lipid melting temperatures with those induced by other proteins suggests that A-FABP behaves like a typical peripheral membrane protein. The degree of membrane interaction correlates directly with the rate of fatty acid transfer, suggesting that contact between A-FABP and membranes is functionally related to its fatty acid transport properties. As expected, the protein exhibits a predominantly β-sheet structure. It was found to aggregate with increasing temperature. With the exception of minor differences between the pure and lipid-associated A-FABP in the 1640−1660 cm^{-1} region, both the protein structure and thermal stability appeared essentially unchanged upon interaction with the lipid.

The mammalian adipocyte functions as a reservoir for triacylglycerol, storing and releasing large amounts of fatty acids (FAs) during regulated cycles of triacylglycerol synthesis and lipolysis (*1*). Adipocyte differentiation is accompanied by dramatic increases in the expression and activity of lipid metabolic enzymes (*2*−*4*) and the 14.1 kDa adipocyte fatty acid-binding protein (A-FABP) (*5*, *6*), also referred to as AP2 and ALBP. It is thought that A-FABP may function as an intracellular transport protein for FA, and thereby be involved in the regulation of cellular lipid metabolism.

Studies of the transfer kinetics of fluorescent anthroyloxy-labeled long-chain fatty acids (AOFA) from A-FABP to model membranes have been used to examine the mechanism and regulation of FA transfer properties of A-FABP *in vitro*. The results have shown that FA movement from A-FABP to membranes does not appear to be regulated by the rate of FA dissociation from the A-FABP-binding site, but rather that FA transfer from A-FABP to membranes may involve direct collisional interactions between the protein and the phospholipid bilayer (*7*). The regulation of the rate of AOFA transfer by the charge characteristics of the acceptor membrane indicates that electrostatic interactions between the A-FABP surface and phospholipid headgroups are important for this interaction (*8*). Neutralization of surface lysine residues using chemical modification resulted in a dramatic decrease in the absolute rate of AOFA transfer to membranes, an insensitivity to the charge attributes of the membranes, and appeared to decrease effective collisional interactions between A-FABP and membranes such that the limiting step in the transfer process becomes the rate of ligand dissociation from the protein (*9*).

As with most other FABPs, A-FABP is typically referred to as a cytosolic protein. FABP purification schemes from various tissues including adipose tissue have used the cytosolic fraction as starting material (*10*, *11*), and immunomicroscopic studies have demonstrated the cytosolic localization of several FABPs (*12*, *13*). Nevertheless, the studies of AOFA transfer kinetics strongly suggest that A-FABP may interact with membranes. The present study was therefore undertaken to directly examine the hypothesis that A-FABP is a membrane-interactive protein.

Fourier transform infrared (FTIR) spectroscopy has been widely utilized for the characterization of lipid phase transitions, and alterations in phase transition properties are used to demonstrate protein−membrane interactions (*14*). The methylene stretching vibrations near 2920 and 2850

† This work was supported by the U.S. Public Health Service through Grants GM 29864 (R.M.), DK38389 (J.S.), and National Research Service Award DK09313 (E.R.S.). A.G. was supported by a grant from the Deutsche Forschungsgemeinschaft (DFG). J.S. is an Established Investigator of the American Heart Association.

‡ Department of Chemistry.

§ Department of Nutritional Sciences.

|| Present address: Department of Radiation Oncology, Emory University, Atlanta, GA 30335.

⊥ Present address: International Speciality Products, Wayne, NJ 07470.

⊗ Abstract published in *Advance ACS Abstracts,* June 15, 1997.

S0006-2960(97)00679-X CCC: $14.00

cm^{-1} are most frequently used for this purpose. The frequencies of these bands shift to higher wavenumbers upon introduction of *gauche* rotamers into the acyl chains (*15*). A second approach to the detection of acyl chain melting phase transitions is based on the fact that the CH_2 wagging bands couple in ordered phases to produce band progressions, the intensity and position of which depend upon the length of the *all-trans* segments involved (*16*, *17*). The introduction of *gauche* rotamers into *all-trans*-polymethylene chains results in a reduction of the length of the residual *all-trans*-polymethylene segments and a weakening of the coupling of the CH_2 wagging vibrations. Therefore, these band progressions disappear upon hydrocarbon chain melting. In addition, IR spectroscopy provides insight into the overall secondary structure of proteins in solution and can be conveniently used to monitor lipid-induced changes in protein structure (*18*−*21*).

The results of the present FTIR study unequivocally demonstrate that the adipocyte fatty acid-binding protein interacts with phospholipid bilayers, and that the rate of FA transfer from A-FABP correlates directly with the degree of protein−membrane interaction. In addition, the sensitive technique of 2D-IR spectroscopy is used to show that the secondary structure (primarily β-sheet) and thermal stability of A-FABP are essentially unchanged upon its interaction with phospholipids.

EXPERIMENTAL PROCEDURES

Materials. Dimyristoylphosphatidylserine (DMPS), egg phosphatidylcholine (EPC), dimyristoylphosphatidylcholine (DMPC), 1-palmitoyl-2-oleoylphosphatidylserine (POPS), 1-palmitoyl-2-oleoylphosphatidylcholine (POPC), heart cardiolipin (CL), tetramyristoylcardiolipin, and 2-[12-(7-nitro-2,1,3-benzoxadiazol-4-yl)amino]dodecanoyl-1-hexadecanoyl-*sn*-glycerophosphocholine (NBD-PC) were obtained from Avanti Polar Lipids (Alabaster, AL) and used as received. 2-(9-Anthroyloxy)palmitic acid (2AP) was from Molecular Probes (Eugene, OR). Recombinant murine A-FABP was purified from an *Escherichia coli* expression system as previously described (Herr et al., 1995). D_2O (isotopic enrichment 99.9%) was obtained from Isotec (Miamisburg, OH).

Sample Preparation and IR Methods. FTIR spectra were collected on a Mattson Instruments Research Series (RS-1) spectrometer equipped with an MCT detector. Multilamellar lipid vesicles were prepared by dispersion in buffer solution (150 mM NaCl, 10 mM K_3PO_4, pH 8.4) or protein-containing buffer solution. For the measurements determining the lipid phase transition, the lipid:protein ratio was 200:1, with a protein concentration of 1.2 mM. Different lipid:protein ratios (50:1 and 25:1) and protein concentrations (0.69 mM) yielded similar results. The A-FABP concentrations used were in the reported range of physiological concentrations of this abundant protein (*22*, *23*). The samples were placed between CaF_2 windows separated with a 25 μm spacer. For the measurements aimed at determination of the protein secondary structure, A-FABP was dissolved in a D_2O buffer at 0.69 mM concentration. For this lower concentration, the spacer had a thickness of 56 μm. The CaF_2 windows enclosing the sample were contained in a thermostated transmission cell (Harrick Scientific, Ossining, NY). Temperature was controlled with a circulating water bath and monitored with a digital thermocouple (Physitemp Instruments, Clifton, NJ). All spectra were obtained at 4 cm^{-1} resolution under N_2 spectrometer purge, by co-addition of 1024 interferograms. The interferograms were apodized with a triangular function and Fourier-transformed with 2 levels of zero-filling, yielding spectra encoded every ≈1 cm^{-1}.

IR Data Reduction Protocols. The precise frequencies of the symmetric methylene stretching [$\nu_s(CH_2)$] modes were determined from second-derivative spectra. The reproducibility within a set of experiments of the observed melting temperature of the lipid was ±0.2 °C, while that of the measured wavenumber was ±0.1 cm^{-1} for a given temperature.

For evaluation of the amide-I band contour, a matching D_2O buffer obtained at exactly the same temperature as the sample spectrum was subtracted from each protein spectrum. The residual H_2O and HOD content of the reference buffer matched exactly the respective concentrations in the sample spectrum, as judged by the intensities of the H_2O and HOD stretching bands centered at ≈3850 and 3420 cm^{-1}, respectively. An exact match is required because the H_2O and HOD bending modes are found in a spectral region which interferes with the amide-I band region. The subtraction factors were 1 ± 0.002, and no base line correction was necessary after subtraction. The second-derivative spectra were obtained by using a 5-data-point Savitzky−Golay smoothing window; i.e., the data were practically unsmoothed.

2D-IR spectra were obtained by subtracting each sample spectrum as described above and cutting the spectra to an appropiate spectral region. As a result of density changes with temperature (resulting in different absorbances), the spectra had to be normalized. In the pure protein cases, all spectra were normalized to the area between 1597 and 1700 cm^{-1}, while in the presence of the lipid this region was extended to 1780 cm^{-1}. The 2D-IR spectra were calculated using a home-written version of the algorithm described by Noda (*24*).

AOFA Transfer from A-FABP to Membranes. The rate of transfer of fatty acid from A-FABP to vesicles was monitored in the same buffer used for FTIR experiments, using the fluorescent anthroyloxy-labeled palmitate analogue 2AP and a resonance energy transfer assay, as described previously (*7*, *8*, *9*). Small unilamellar vesicles (SUV), composed of 25 mol % of the indicated phospholipid, 65 mol % EPC, and 10 mol % of the quencher NBD-PC, were prepared by sonication and ultracentrifugation (*25*).

RESULTS

Diacylphosphatidylserine/A-FABP. In Figure 1, the temperature dependence of the symmetric methylene stretching vibrations [$\nu_s(CH_2)$] of the dimyristoylphosphatidylserine (DMPS) and 1-palmitoyl-2-oleoylphosphatidylserine (POPS) acyl chains is shown for the pure lipid and for lipid in the presence of A-FABP. The sharp gel/liquid-crystalline phase transition of pure DMPS (Figure 1a) was found at the expected temperature (35 °C) (*26*). In the presence of A-FABP, the $\nu_s(CH_2)$ wavenumbers are slightly elevated for all temperatures, and the cooperativity of the lipid shifts approximately 1−2 °C to lower temperatures (repeats of the individual experiments are essentially superimposible). A more dramatic change is observed for POPS (Figure 1b), where the phase transition of the lipid shifts by ≈5 °C. This

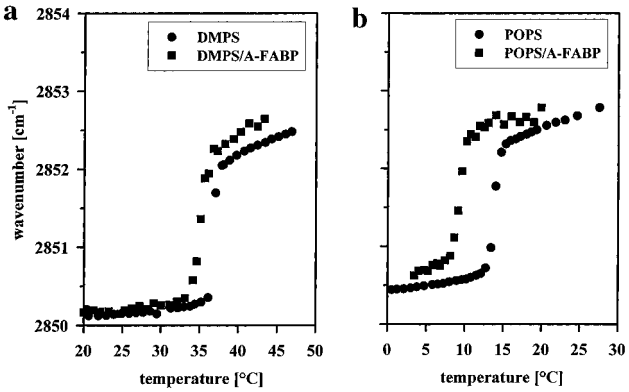

FIGURE 1: Frequencies of the $\nu_s(CH_2)$ vibrations (±0.1 cm^{-1}) *vs* temperature for DMPS and POPS multilamellar vesicles for the pure lipid and in the presence of A-FABP.

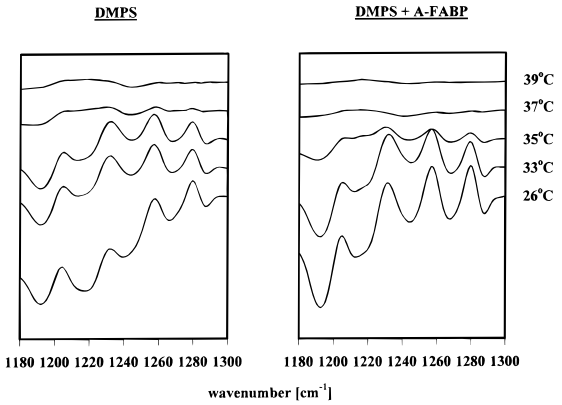

FIGURE 2: Methylene wagging progression bands for pure DMPS and in the presence of A-FABP at different temperatures.

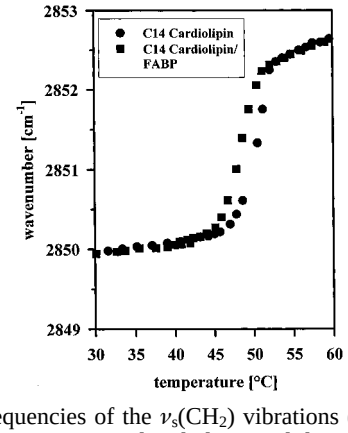

FIGURE 3: Frequencies of the $\nu_s(CH_2)$ vibrations (±0.1 cm^{-1}) *vs* temperature for tetramyristoylcardiolipin multilamellar vesicles for the pure lipid and in the presence of A-FABP.

shift of the phase transition can also be demonstrated by monitoring the coupled methylene progression modes. In general, these coupled modes are exclusively found for an *all-trans*-polymethylene chain and disappear upon introduction of *gauche* conformers. In Figure 2, the coupled CH_2 progression modes are displayed for DMPS in the presence and absence of A-FABP. It is observed that the progression bands vanish at around 35 °C in the presence of A-FABP, while in the case of pure DMPS the progression bands are still present at this temperature and disappear around 37 °C.

Cardiolipin/A-FABP. In Figure 3, the CH_2 stretching frequencies are displayed *vs* temperature for tetramyristoylcardiolipin alone and in the presence of A-FABP. For the pure lipid, the melting temperature as inferred from the CH_2 stretching vibrations is found at approximately 52 °C, in agreement with the literature value (*26*). The coupled methylene progression bands are very strong and vanish at this temperature (not shown). In the presence of A-FABP, the melting point is lowered by approximately 2 °C (Figure 3), which is also found by analyzing the methylene progression bands (data not shown).

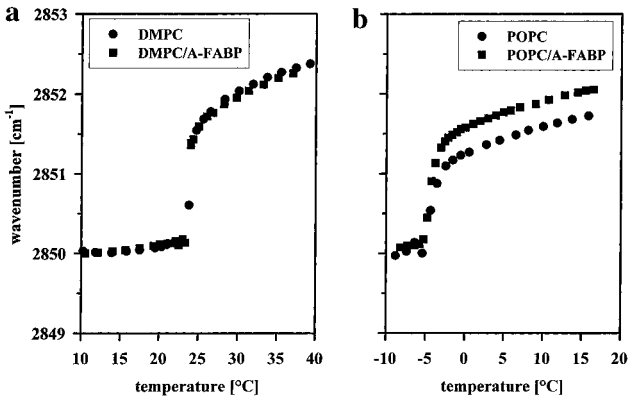

FIGURE 4: Frequencies of the $\nu_s(CH_2)$ vibrations (±0.1 cm^{-1}) *vs* temperature for DMPC and POPC multilamellar vesicles for the pure lipid and in the presence of A-FABP.

Diacylphosphatidylcholine/A-FABP. AOFA transfer studies had suggested that A-FABP interactions with PC membranes would be of lesser magnitude than those with membranes containing acidic phospholipids. It was therefore of interest to examine the effects of A-FABP on bilayers containing exclusively PC headroups. In Figure 4a, the CH_2 stretching frequencies for pure dimyristoylphosphatidylcholine (DMPC) are compared with the respective values obtained in the presence of A-FABP. It is found that the data points superimpose within the accuracy of the method, indicating a considerably weaker interaction of A-FABP with DMPC than with DMPS. The dependence of lipid−protein interaction on the lipid headgroup is examined for the unsaturated lipid 1-palmitoyl-2-oleoylphosphatidylcholine (POPC). In Figure 4b, the methylene stretching frequencies for pure POPC are compared to those in the presence of A-FABP, which were obtained by cooling the sample in steps of 0.5 °C to −10 °C. It is found that the phase transition for both samples is located at ≈−3.5 °C. At temperatures higher than the transition temperature, the wavenumbers for the $\nu_s(CH_2)$ vibration are sligthly elevated in the presence of A-FABP in comparison to the pure lipid case. Although this indicates a minor interaction between POPC and A-FABP, it is considerably smaller than in the case of POPS.

Comparison of A-FABP and Acetylated A-FABP. Since previous studies showed a large decrease in AOFA transfer rate from A-FABP following neutralization of surface lysine residues, we compared the effects of acetylated and native A-FABPs on POPS vesicles. In Figure 5, $\nu_s(CH_2)$ for POPS in the presence of acetylated A-FABP are compared to those for the pure lipid and in the presence of unmodified A-FABP. It is found that the phase transition of POPS in the presence of the acetylated A-FABP is shifted to higher temperatures (2−3 °C) than in the presence of native A-FABP. However, the transition is still found at lower temperatures compared with the pure lipid.

Effect of Acceptor Membrane Composition on AOFA Transfer Rate from A-FABP. To determine whether the apparent degree of A-FABP−membrane interaction cor-

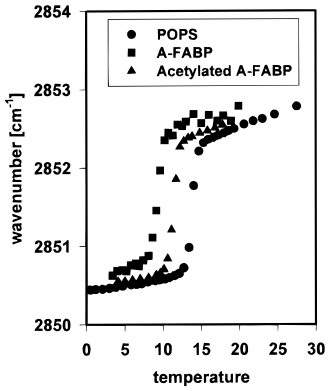

FIGURE 5: Frequencies of the $\nu_s(CH_2)$ vibrations (± 0.1 cm^{-1}) *vs* temperature for pure POPS and in the presence of A-FABP or acetylated A-FABP.

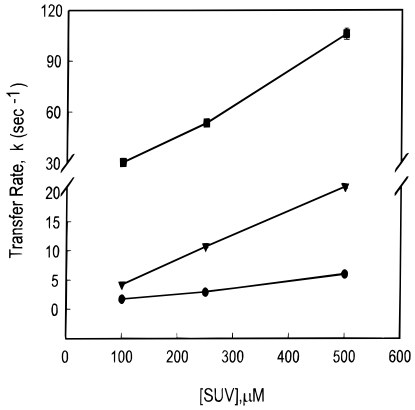

FIGURE 6: Transfer at 24 °C of 1 mM 2AP from 10 mM A-FABP to SUV composed of 25 mol % POPC (●), POPS (▼), or CL (■). Error bars which are not visible are of very small magnitude.

relates with the rate of FA transfer, we monitored the movement of 2AP from A-FABP to increasing concentrations of vesicles containing 25 mol % of POPC, POPS, or heart CL, under conditions similar to those used in the FTIR experiments. The results in Figure 6 show that for all three vesicle types, the rate of AOFA transfer increased in direct proportion to the membrane phospholipid concentration. This is in agreement with our previous results (*8*), and suggests that FA transfer from A-FABP to all these vesicles occurs via collisional interaction of the protein with the membrane. It is noteworthy that the absolute rate of 2AP transfer from A-FABP to membranes is in the order of CL > PS > PC. A comparison with the FTIR data shows that the degree of membrane interaction, as inferred from the extent of the decrease in phospholipid T_m, is directly related to the rate of 2AP transfer. Comparisons between phospholipids with different headgroups but the same acyl chain composition demonstrate that A-FABP interacts more strongly with acidic phospholipid membranes than with zwitterionic membranes. For instance, the ΔT_m for POPS in the presence of A-FABP is 5 °C whereas for POPC it is barely detectable (Figures 1b and 4b). A comparison of these results with the corresponding dioleoyldipalmitoylcardiolipin was not done due to unavailability of the lipid. In addition, the T_m for tetraoleoylcardiolipin is too low to measure the influence of A-FABP on the melting transition of this lipid. The ΔT_m for DMPC in the presence of A-FABP is barely discernible, but is approximately 1.5 °C for DMPS and 2 °C for tetramyristoyl-CL vesicles (Figures 1a, 3, and 4a).

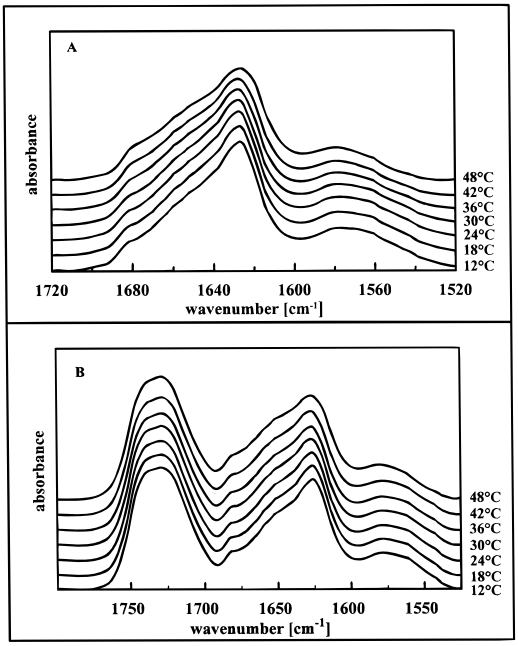

FIGURE 7: (A) A-FABP spectrum *vs* temperature in the range 1520−1720 cm^{-1}. (B) A-FABP in the presence of tetraoleoylcardiolipin (lipid:protein ratio 50:1) *vs* temperature in the range 1520−1800 cm^{-1}. The protein concentration is in both cases 0.69 mM. In both cases, the buffer solution-subtracted spectra are shown.

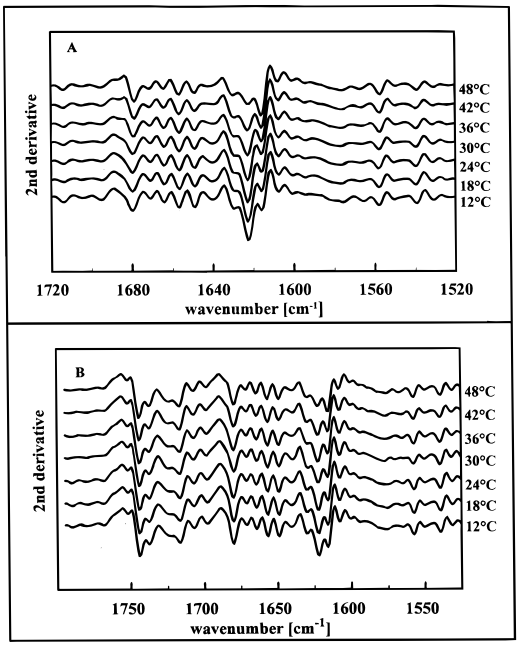

FIGURE 8: Second-derivative spectra of pure A-FABP (A) and in the presence of tetraoeloylcardiolipin (B). Protein concentration was 0.69 mM, and lipid:protein ratio was 50:1.

Secondary Structure of the Protein at Different Temperatures. In Figure 7, the IR spectra of the pure protein at different temperatures are compared to those in the presence of tetraoleoylcardiolipin, while in Figure 8 the corresponding second-derivative spectra are displayed. At low temperatures, the main component within the amide-I band envelope is found at 1626 cm^{-1}, while at higher temperatures this band is diminished and the component at 1618 cm^{-1} increases. Along with these two bands, a third band is found at 1631 cm^{-1}, which appears to be quite stable over the temperature range studied. A strong band in the region 1620−1635 cm^{-1} accompanied by a somewhat weaker band located around

1683 cm^{-1} is indicative of a β-sheet secondary structure. However, it is not clear why in the present case two bands are found in the 1620−1635 cm^{-1} region; this issue will be addressed below. The band at 1618 cm^{-1} was assigned to an aggregated or intermolecular β-sheet (*27*); i.e., the main denaturation process of A-FABP upon heating is obviously aggregation rather than unfolding. Comparison of this thermal denaturation process with chemical denaturation by 6 M [^{13}C]urea (data not shown) revealed no differences; i.e., a very strong band at 1618 cm^{-1} was again observed. It should be noted that in both cases, i.e., thermal and chemical denaturation, no strong bands appear in the 1640−1650 cm^{-1} region, which indicates that the amount of random coil is virtually unchanged upon denaturation.

The band found at 1674 cm^{-1} (Figure 8) is most likely due to β-turns (*28*), while the structural origin of the other bands marked in Figure 8 (1641, 1652, 1660, 1667 cm^{-1}) cannot be unequivocally assigned. However, the bands in the region 1640−1660 cm^{-1} can be attributed to random coil and helical structures (*28*). Comparison of the amide-I region for the protein in the absence and presence of the lipid reveals no major changes in the predominant β-sheet structure of the protein upon binding to the lipid. In particular, the temperature dependence of the bands at 1626 and 1618 cm^{-1} is essentially the same in the presence and absence of the lipid. Careful subtraction of normalized spectra (data not shown) revealed small differences in the region 1640−1660 cm^{-1} between the pure and lipid-associated protein, which might be attributable to changes in the helical and/or random coil content of the protein upon binding to the lipid. Considering that the amide-I band contour in the presence of the lipid is disturbed by the nearby carbonyl band, the changes appear to be too small to be unambiguously assigned. However, it should be noted that these differences were also found for lipid:protein ratios as small as 20:1, where the influence of the carbonyl band is strongly diminished in comparision to the case displayed in Figure 7B.

Denaturation processes and changes in the protein secondary structure due to interaction with lipids are most often addressed by curve-fitting the amide-I band envelopes and subsequently comparing the temperature dependence of the subband intensities (*19*). However, in this and other cases, this approach is not feasible because the amide-I band is very broad, featureless, and overlapped with side chain bands as well as the amide-II band envelope (the latter indicates that the protein is only partially H/D-exchanged). Furthermore, in the presence of lipid, the amide-I band is overlapped with the lipid carbonyl band. This results in the fact that whereas for the pure protein the spectral region between ≈1500 and 1700 cm^{-1} has to be analyzed, in the presence of the lipid this region must be extended to 1800 cm^{-1}. Deriving a unique mathematical solution for such a large assembly of bands was not possible. Therefore, to obtain a more detailed picture about the structural processes which take place upon denaturation of A-FABP, the 2D-IR algorithm (introduced below) was employed.

2D-IR Spectra of the FABP Protein. The 2D-IR algorithm is a relatively new method introduced by Noda (*24*) which spreads the IR spectrum into a second dimension, thereby enhancing the spectral resolution (resolving overlapped band contours). The method permits one to determine whether bands change in a correlated or an uncorrelated manner, and furthermore allows one to distinguish between shifting bands and bands changing intensities (*29*). Briefly, 2D-IR plots are generated by applying an external perturbation to the system under investigation, resulting in a series of spectra with changing properties. In the present case, the external perturbation was the changing temperature. The spectra are combined in one intensity matrix, which is subsequently Fourier-transformed. The intensity variations at each wavenumber position are then correlated in a pairwise fashion. Two 2D-IR plots are thereby obtained, one of which exhibits cross-peaks for bands which change in a correlated fashion, while the other plot displays cross-peaks for bands which change in an uncorrelated fashion upon perturbation. The latter generally exhibits stronger resolution enhancement, which might be useful for confirmation of uncertain spectral features. However, the interpretation of the origin of the cross-peaks in the correlated 2D-IR plot (Figure 9) is much more straightforward than for the respective uncorrelated plot (*29*). The solid and dashed contour lines in the 2D plot represent positive and negative 2D peaks, respectively. Correlated peaks occur at the wavenumber positions which intersect along the diagonal when orthogonal X and Y projections are made.

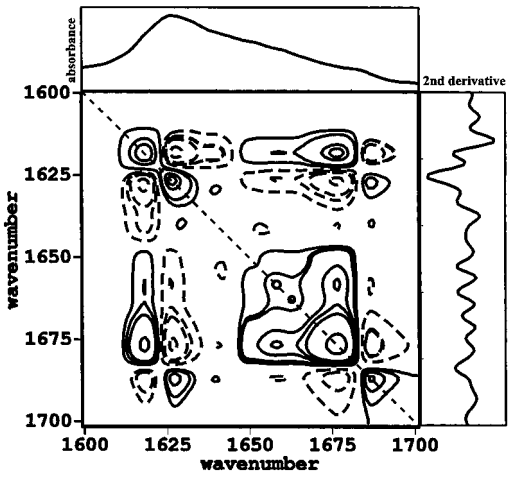

FIGURE 9: 2D-IR correlated (synchronous) plot for pure A-FABP (0.69 mM) in the temperature range 12−42 °C (16 spectra). The spectra were normalized to the area 1597−1700 cm^{-1} prior to the calculation of the 2D plot. At the top of the contour plot the original spectrum (14 °C) is given, while at the right side the respective second-derivative spectrum is displayed. Solid contour and dashed lines mark positive and negative peaks, respectively. The diagonal of the plot is marked by a dashed line.

The plot was generated for 16 spectra obtained between 12 and 42 °C, i.e., before the major transition from a β-sheet to an aggregate takes place (see Figure 8). If the whole temperature range is chosen for generating the 2D plot, the 2D peaks for the bands located at 1618, 1626, 1675, and 1683 cm^{-1} become so dominant that no other features are discernible in the plot. Generally the 2D plot exhibits autopeaks at the diagonal, which are due to the correlation of an individual peak with itself. Large autopeaks are observed for bands which undergo strong intensity changes, while weak autopeaks are found for minor intensity changes (*24*, *29*). In the present case, some autopeaks are not found due to superimposition by the larger 2D peaks. Negative cross-peaks indicate that the two correlated band intensities change in opposite fashion; i.e., the intensity for one band decreases in the course of the perturbation, while the intensity

for the other band increases. This can be exemplified for the negatively correlated 1626/1618 cm^{-1} pair, where the 1D (normal) IR spectra show that the band at 1626 cm^{-1} decreases with increasing temperature, while the opposite is found for the band at 1618 cm^{-1}. The second strong feature in the 2D plot is the negative correlation between the bands at 1683 and 1675 cm^{-1}. In turn, positive correlations are found for the pairs 1626/1683 cm^{-1} and 1618/1675 cm^{-1}. Since the band at 1675 cm^{-1} most likely represents β-turns, the amount of β-turns obviously increases upon denaturation; i.e., aggregation changes the β-sheet within the A-FABP structure. Although already present at lower temperatures, the main aggregation process starts above ≈44 °C. The aggregation of the protein is irreversible. Such aggregation behavior was also reported for other proteins with predominantly β-sheet structure (*27*).

The band at 1631 cm^{-1} changes only slightly and shows a positive cross-peak with the band at 1640 cm^{-1}, the latter possibly representing a random coil structure. Since the 1640 cm^{-1} band is positively correlated with the band at 1683 cm^{-1}, which is decreasing in intensity upon heating (see above), the bands at 1640 and 1631 cm^{-1} are obviously decreasing as well, although the changes are quite small. It should be noted that no strong cross-correlations are discernible for the 1631 cm^{-1} band with the β-sheet bands located at 1618, 1626, and 1683 cm^{-1}, which might indicate that this band does not represent a β-sheet. Comparison of the 2D plots in the absence and presence (not shown) of the lipid reveals no major differences; i.e., A-FABP stability (resistance to aggregation) is similar.

DISCUSSION

These studies strengthen the hypothesis that the adipocyte FABP is a membrane-interactive protein, as predicted by studies of the kinetics of fluorescent fatty acid transfer to model phospholipid vesicles (*7*, *8*, *9*). The large decreases in the lipid phase transition temperatures of anionic vesicles in the presence of A-FABP demonstrate the strength of these interactions. The direct correlation between the degree of A-FABP−membrane interaction and the rate of AOFA transfer to membranes indicates further that the rate of FA transfer from A-FABP to membranes is governed by effective collisional interactions between the protein and membranes.

The magnitude of the decrease in the transition temperatures (1−5 °C) observed during the interaction of A-FABP with the charged phospholipids is comparable to those measured for the interaction of peripheral membrane proteins with zwitterionic lipids. For example, Vincent and Levin (*30*) have shown that the transition temperature of DPPC is lowered by about 4 °C upon its interaction with cytochrome *c*, as measured from a variety of Raman spectral parameters, and the transition is slightly broadened. In addition, electrostatic interactions between a soluble, positively-charged cardiotoxin and negatively charged dimyristoylphosphatidate induced extensive disordering of the lipid gel phase, and completely abolished the phase transition (*31*). The penetration of the toxin into the apolar regions of the bilayer was suggested. It is also of interest that despite the large shift in the melting temperature observed for anionic membranes in the presence of A-FABP, the cooperativity of the gel to liquid-crystalline phase transition, as inferred from the slope of the curve of $\nu_s(CH_2)$ *vs* temperature, was altered minimally at most (e.g., Figure 1b). This suggests that A-FABP does not penetrate deeply, if at all, into the hydrophobic core of the membrane. Nevertheless, the data are consistent with protein interaction at the membrane surface, with the A-FABP−membrane interaction likely governed by electrostatic forces. This is evidenced by the magnitude of the A-FABP effect on acidic membranes relative to zwitterionic membranes, and by the substantial decrease in interaction observed for acetylated A-FABP, in which the 14 basic lysine residues on the surface of the protein are neutralized (*9*). Furthermore, in other studies, we have found that A-FABP−membrane interactions are interrupted by salt concentrations of ≥150−200 mM.[1]

In spite of the above, the present study shows that properties of the hydrophobic core of the membrane can also influence the A-FABP−membrane interaction. It is seen that for a given headgroup, a difference in acyl chain composition can substantially affect the degree of A-FABP−membrane interaction; the ΔT_m for POPS is considerably larger than the ΔT_m for DMPS (Figure 1). This might be a direct effect of A-FABP interaction with the acyl chain region of the bilayer, but might also arise as a secondary result of changes in headgroup conformation and packing, caused by differences in acyl chain saturation between POPS and DMPS (*32*). In addition, although the absolute rate of AOFA transfer to PC membranes is much slower than the transfer rate to membranes containing anionic phospholipids (Figure 6), the mechanism of transfer to these membranes is still likely to involve protein−membrane interactions (*8*). Although this too may suggest that forces in addition to electrostatic interactions are involved in the A-FABP−membrane-binding complex, it must be recalled that the PC headgroup, although possessing a net charge of zero, contains ionized phosphate and amino groups which could interact with charged residues on the A-FABP surface. Thus, although at present it is not known whether A-FABP interacts solely with the surface of the bilayer or whether it may penetrate slightly into the membrane core, it is clear that electrostatic interactions are dominant in this peripheral membrane association.

High-resolution structures of several members of the FABP family have been obtained by crystallographic analysis (*33*). All have been shown to be composed of 10 antiparallel β-strands which form a barrel-like structure containing the FA-binding cavity. The IR spectroscopic findings in this work are in agreement with these structures. The barrel is capped by two short α-helical segments which are hypothesized to be part of a "portal" domain, where FA enters and exits the cavity. Site-directed mutagenesis studies of the heart FABP (HFABP) demonstrated that alterations in the charge characteristics of the α-I helix influenced both the absolute rate of AOFA transfer to membranes and the regulation of transfer by acceptor membrane charge (*34*). Additionally, mutations which eliminated positive charges in the α-II helix and β-2 turn, the latter also in the portal region, were found to modulate the process of FA transfer from HFABP to membranes (*34*). The apparent importance of the portal domain, and of the two helical segments in particular, in AOFA transfer from A-FABP has also been recently demonstrated.[2] The α-I helix of A-FABP is

[1] E. R. Smith and J. Storch, unpublished observations.
[2] H.-L. Liou and J. Storch, unpublished observations.

amphipathic, and such structures are well-known to form peripheral interactions with acidic membranes (*35*). We therefore hypothesize that the helical/portal region of A-FABP is centrally involved in the interaction of the protein with membranes. Interestingly, recent studies of an intestinal FABP (IFABP) mutant, in which the helical domain has been eliminated, demonstrate that while overall protein folding is minimally affected, the ligand-binding properties are modified in such a way as to suggest that the helical domain is involved in the FA transfer process (*36*, *37*). The minor differences between the pure and phospholipid-associated A-FABP in the 1640−1660 cm^{-1} region might indicate changes in the portal region of A-FABP upon binding. However, due to the uncertainties in the data processing discussed above, this question cannot be resolved conclusively. It should be noted that denaturation of A-FABP does not result in random coil formation but leads to an increased aggregation. The thermal stability of AFBP was not affected by the presence of anionic lipids.

The present studies demonstrate clearly that A-FABP interacts with phospholipid bilayers. As evidenced by immunocytochemical localization studies, most FABPs are thought to be cytoplasmically localized (*12*, *13*, *39*), although data for A-FABP have not been reported. In this regard, it is of interest that the myelin P2 protein, which shares >60% sequence identity with A-FABP, has been shown to have the properties of a classical "extrinsic" membrane protein. Ultrastructural studies of myelin P2 in Schwann cells demonstrated a peripheral membrane localization, and biochemical studies showed that the protein could be extracted from membranes by alterations in buffer ionic strength (*39*, *40*). It is possible, therefore, that the homologous A-FABP may be acting *in vivo* to target the delivery and/or extraction of unesterified fatty acids to and from their intracellular membrane-bound sites of lipid biosynthesis, oxidation, or transmembrane flux.

ACKNOWLEDGMENT

We acknowledge the excellent technical assistance of Ana Monroy.

REFERENCES

1. Hirsch, J., Fried, S. K., Edens, N. K., and Leibel, R. L. (1989) The fat cell. *The Medical Clinics of North America* (Bray, G., Ed.) Vol. 73, 83−96, W. B. Sauders Co., Philadelphia, PA.
2. Coleman, R. A., Reed, B. C., Mackall, J. C., Student, A. K., Lane, M. D., and Bell, R. M. (1978) *J. Biol. Chem. 253*, 7256−7261.
3. Bernlohr, D. A., Bolanowski, M. A., Kelly, T. J., and Lane, M. D. (1985) *J. Biol. Chem. 260*, 5563−5567.
4. Carnicero, H. H. (1984) *J. Biol. Chem. 259*, 3844−3850.
5. Bernlohr, D. A., Angus, C. W., Lane, M. D., Bolanowski, M. A., and Kelly, T. J. (1984) *Proc. Natl. Acad. Sci. U.S.A. 81*, 5468−5472.
6. Spiegelman, B. M., Frank, M., and Green, H. (1983) *J. Biol. Chem. 258*, 10083−10089.
7. Wootan, M. G., and Storch, J. (1993) *Biochemistry 32*, 8622−8627.
8. Wootan, M. G., and Storch, J. (1994) *J. Biol. Chem. 269*, 10517−10523.
9. Herr, F. M., Matarese, V., Bernlohr, D. A., and Storch, J. (1995) *Biochemistry 34*, 11840−11845.
10. Matarese, V., and Bernlohr, D. A. (1988) *J. Biol. Chem. 263*, 14544−14551.
11. Ockner, R. K., and Manning, J. A. (1974) *J. Clin. Invest. 54*, 326−338.
12. Shields, H. M., Bates, M. L., Bass, N. M., Best, C. J., Alpers, D. H., and Ockner, R. K. (1986) *J. Lipid Res. 27*, 549−557.
13. Suzuki, T., and Ono, T. (1987) *J. Pathol. 153*, 385−394.
14. Lewis, R. N. A. H., and McElhaney, R. (1996) in *Infrared Spectroscopy of Biomolecules* (Mantsch, H. H., and Capman, D., Eds.) Wiley Interscience, New York.
15. Snyder, R. G. (1967) *J. Chem. Phys. 47*, 1316−1360.
16. Senak, L., Moore, D. J., and Mendelsohn, R. (1992) *J. Phys. Chem. 96*, 2749−2754.
17. Moore, D. J., and Mendelsohn, R. (1994) *Biochemistry 33*, 4080−4085.
18. Braiman, M. S., and Rothschild, K. J. (1988) *Annu. Rev. Biophys. Biophys. Chem. 17*, 541−570.
19. Haris, P. I., and Chapman, D. (1992) *Trends Biochem. Sci. 17*, 328−333.
20. Briggs, M. S., Cornell, D. G., Dluhy, R., and Gierasch, L. M. (1986) *Science 233*, 206−208.
21. El-Jastami, R., and Lafleur, M. (1997) *Biochim. Biophys. Acta 1324*, 151−158.
22. Baxa, C. A., Sha, R. S., Buelt, M. K., Smith, A. J., Matarese, V., Chinander, L. L., Boundy, K. L., and Bernlohr, D. A. (1989) *Biochemistry 28*, 8683−8690.
23. Spiegelman, B. M., and Green, H. (1980) *J. Biol. Chem. 255*, 8811−8818.
24. Noda, I. (1993) *Appl. Spectrosc. 47*, 1329−1336.
25. Huang, C., and Thompson, T. E. (1974) *Methods Enzymol. 32*, 485−489.
26. Cevc, G., and Marsh, D. (1987) *Phospholipid Bilayers*, 2nd ed., Wiley, New York.
27. Van Stokkum, I. H. M., Linsdell, H., Hadden, J. M., Haris, P. I., Chapman, D., and Bloemendal, M. (1995) *Biochemistry 34*, 10508−10518.
28. Susi, H., and Byler, D. M. (1986) *Methods Enzymol. 130*, 290−311.
29. Gericke, A., Gadaleta, S. J., Brauner, J. W., and Mendelsohn, R. (1996) *Biospectroscopy 2*, 341−351.
30. Vincent, J. S., and Levin, I. W. (1988) *Biochemistry 27*, 3438−3446.
31. Desormeaux, G., Laroche, P. E., Bougis, G., and Pezolet, M. (1992) *Biochemistry 31*, 12173−12182.
32. Jones, M. N., and Chapman, D. (1994) *Micelles, Monolayers and Biomembranes*, Wiley, New York.
33. Banaszak, L., Winter, N., Xu, Z., Bernlohr, D. A., Cowan, S., and Jones, T. A. (1994) *Adv. Protein Chemistry 45*, 89−151.
34. Herr, F. M., Aronson, J., and Storch, J. (1996) *Biochemistry 35*, 1296−1303.
35. Anantharamaiah, G. M., Jones, M. K., and Segrest, J. P. (1993) in *The Amphipathic Helix* (Epand, R. M., Ed.) p 110, CRC Press, Boca Raton, FL.
36. Cistola, D. P., Kim. K., Rogl, H., and Frieden, C. (1996) *Biochemistry 35*, 7559−7565.
37. Kim, K., Cistola, D. P., and Frieden, C. (1996) *Biochemistry 35*, 7553−7558.
38. Iseki, S., Kondo, H., Hitomi, M., and Ono, T. (1988) *Histochemistry 89*, 317−322.
39. Trapp, B. D., Dubois-Dalcq, M., and Quarles, R. H. (1984) *J. Neurochem. 43*, 944−948.
40. Uyemura, K., Kato-Yamanaka, T., and Kitamura, K. (1977) *J. Neurochem. 29*, 61−68.

BI970679S